Gradient Discretization of Hybrid Dimensional Darcy Flows in Fractured Porous Media

Konstantin Brenner[1], Maya Groza[1], C. Guichard[2], Gilles Lebeau[1], Roland Masson[1]

[1] LJAD, Université Nice Sophia Antipolis, and team Coffee INRIA Sophia Antipolis
[2] LJLL, Université Paris VI

Séminaire de l'équipe EDP-MOISE-MGMI, LJK Grenoble
26 février 2015

Outline

- Darcy flows in Discrete Fractured Networks (DFN)
- Gradient scheme framework
- VAG and HFV schemes
- Two phase Darcy flows in DFN

Discrete Fracture Network (DFN)

- Full domain: $\Omega \subset \mathbb{R}^d$, $d = 2, 3$
- Discrete Fracture Network: $\Gamma = \bigcup_{i \in I} \Gamma_i$
- Matrix domain: $\Omega \setminus \overline{\Gamma}$
- $\Sigma = \bigcup_{i \neq j} \partial\Gamma_i \cap \partial\Gamma_j$
- $\Sigma_0 = \partial\Gamma \cap \partial\Omega$
- $\Sigma_N = \partial\Gamma \setminus \partial\Omega$

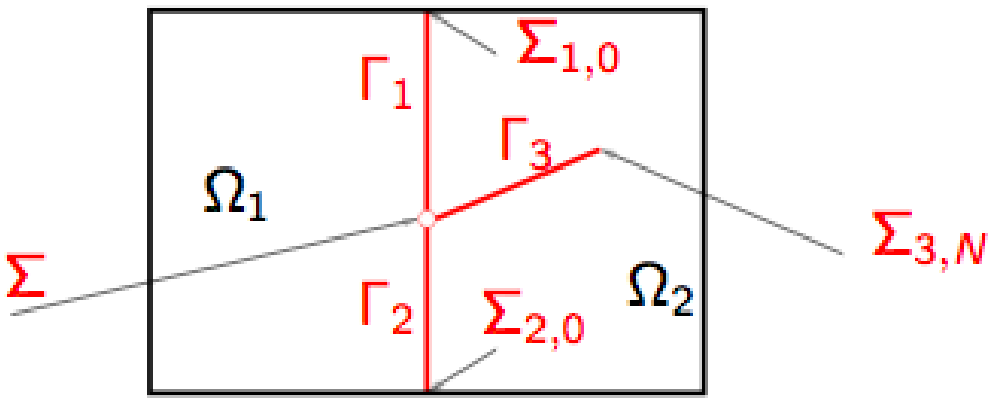

Hybrid dimensional models for DFN [Jaffré et al 2002]

- Integration in the fracture width $d_f << \text{diam}(\Omega)$
  - $d-1$ dimensional model in the fracture
- Continuous pressure assumption at the interface
  - $u^+ = u^- = u_f = \gamma u$ on Γ
    - it assumes $\dfrac{\mathbf{K}_{f,n}}{d_f} >> \dfrac{\mathbf{K}_m}{\text{diam}(\Omega)}$
- Pressure continuity and flux conservation is assumed at fracture intersections

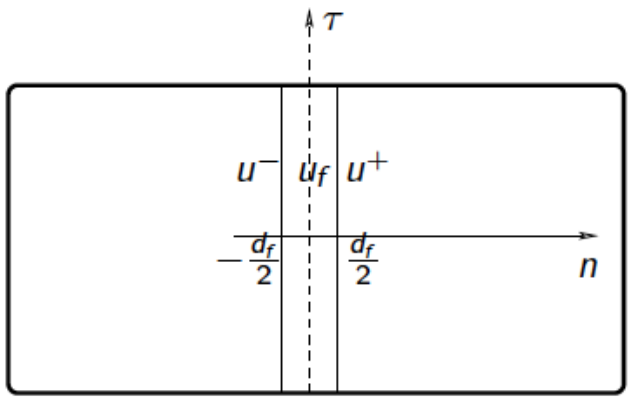

Hybrid dimensional models for Darcy flows in DFN: function spaces

Pressure space V^0: continuous at the matrix fracture and fracture fracture interfaces

$\gamma : H^1(\Omega) \to L^2(\Gamma)$ trace operator

$V^0 = \{v \in H^1_0(\Omega)$ such that $\gamma v \in H^1(\Gamma), \gamma v = 0$ on $\partial\Omega \cap \Gamma\}$,

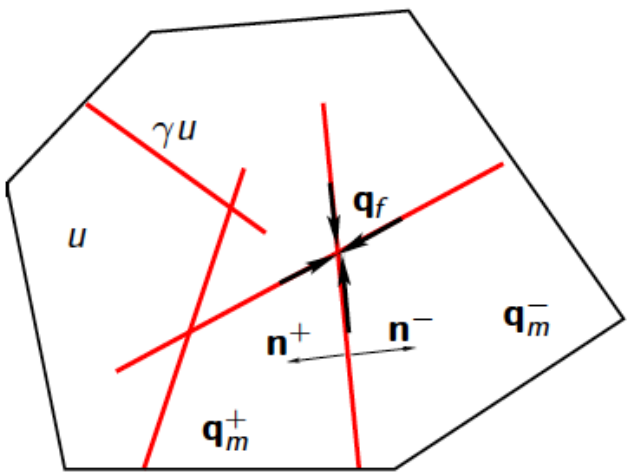

Hybrid dimensional models for Darcy flows in DFN: function spaces

Matrix and fracture flux space W:

$$\mathbf{W} = \left\{ \begin{array}{l} \mathbf{q}_m \in H_{\mathrm{div}}(\Omega \setminus \overline{\Gamma}), \\ \mathbf{q}_f \in L^2(\Gamma)^{d-1}, \\ \text{ such that } \mathrm{div}_\tau(\mathbf{q}_f) + \mathbf{q}_m^+ \cdot \mathbf{n}^+ + \mathbf{q}_m^- \cdot \mathbf{n}^- \in L^2(\Gamma), \\ \text{ and normal flux conservation of } \mathbf{q}_f \text{ at } \Sigma \setminus \Sigma_0 \text{ in a weak sense} \end{array} \right\},$$

Jump of the matrix normal flux on Γ: $\mathbf{q}_m^+ \cdot \mathbf{n}^+ + \mathbf{q}_m^- \cdot \mathbf{n}^-$

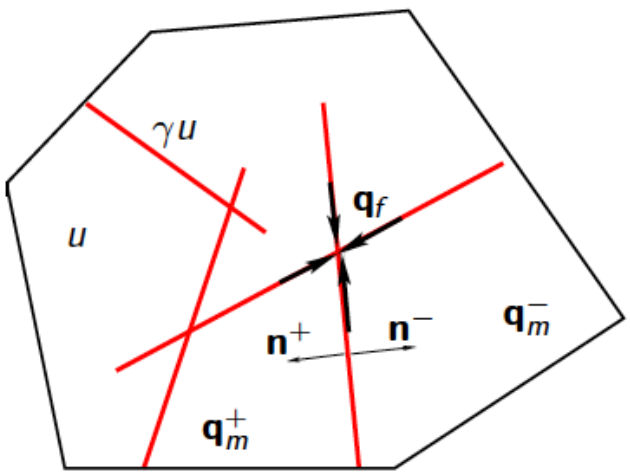

Main functional result: smooth function subspaces are dense in V^0 and $\mathbf{W}$

Hybrid dimensional models for Darcy flows in DFN

Find $u \in V^0$, $(\mathbf{q}_m, \mathbf{q}_f) \in \mathbf{W}$ such that:

$$\begin{cases} \operatorname{div}(\mathbf{q}_m) = h_m & \text{on } \Omega \setminus \overline{\Gamma}, \\ \operatorname{div}_\tau(\mathbf{q}_f) + \mathbf{q}_m^+ \cdot \mathbf{n}^+ + \mathbf{q}_m^- \cdot \mathbf{n}^- = d_f h_f & \text{on } \Gamma, \\ \mathbf{q}_m = -\mathbf{K}_m \nabla u & \text{on } \Omega \setminus \overline{\Gamma}, \\ \mathbf{q}_f = -d_f \mathbf{K}_f \nabla_\tau \gamma u & \text{on } \Gamma, \end{cases}$$

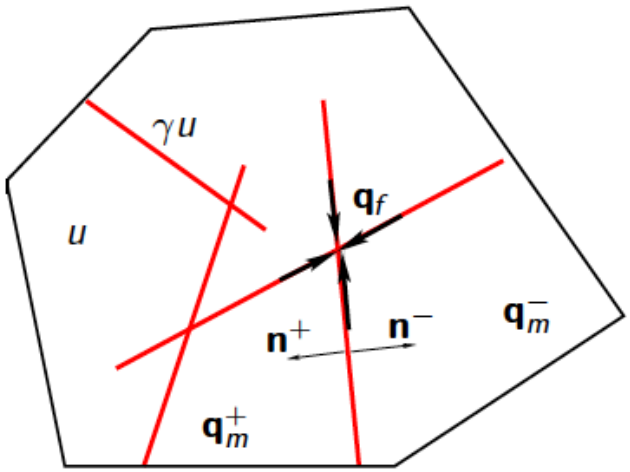

Variational formulation in V^0

The weak formulation amounts to find $u \in V^0$ such that for all $v \in V^0$ one has:

$$\int_\Omega \mathbf{K}_m \nabla u \cdot \nabla v \; d\boldsymbol{x} + \int_\Gamma d_f \mathbf{K}_f \nabla_\tau \gamma u \cdot \nabla_\tau \gamma v \; d\tau(\boldsymbol{x})$$

$$= \int_\Omega h_m \; v \; d\boldsymbol{x} + \int_\Gamma d_f h_f \; \gamma v \; d\tau(\boldsymbol{x}).$$

Discretization: state of the art

- MFE or MHFE: Jaffré et al 2002, Firoozabadi 2008
- TPFA: Karimi-Fard et al 2004
- CVFE: Bastian et al 2006, Firoozabadi et al 2007
- XFEM type methods: Formaggia, Scotti et al 2012
- MPFA: Faille et al, Nordbotten et al, 2012, Edwards 2014
- ...

Our contributions:

- Extension of the Gradient scheme framework (Eymard et al 2010) to DFN models
- Convergence proof for single and two phase flow models
- Vertex Approximate Gradient (VAG) and Hybrid Finite Volume (HFV) discretizations

Gradient discretization framework: non conforming discretization

Vector space of discrete unknowns: $X_{\mathcal{D}}^0$

- Matrix and fracture gradient reconstruction operators
  - $\nabla_{\mathcal{D}_m} : X_{\mathcal{D}}^0 \to L^2(\Omega)^d$
  - $\nabla_{\mathcal{D}_f} : X_{\mathcal{D}}^0 \to L^2(\Gamma)^{d-1}$
- Matrix and fracture function reconstruction operators:
  - $\Pi_{\mathcal{D}_m} : X_{\mathcal{D}}^0 \to L^2(\Omega)$
  - $\Pi_{\mathcal{D}_f} : X_{\mathcal{D}}^0 \to L^2(\Gamma)$

Assumption: $\|u_{\mathcal{D}}\|_{\mathcal{D}} := \|\nabla_{\mathcal{D}_m} u_{\mathcal{D}}\|_{L^2(\Omega)^d} + \|\nabla_{\mathcal{D}_f} u_{\mathcal{D}}\|_{L^2(\Gamma)^{d-1}}$ is a norm on $X_{\mathcal{D}}^0$

Gradient discretization of the hybrid dimensional Darcy flow model

$u_{\mathcal{D}} \in X_{\mathcal{D}}^0$ such that for all $v_{\mathcal{D}} \in X_{\mathcal{D}}^0$ one has

$$\int_\Omega \mathbf{K}_m \nabla_{\mathcal{D}_m} u_{\mathcal{D}} \cdot \nabla_{\mathcal{D}_m} v_{\mathcal{D}} \, d\boldsymbol{x} + \int_\Gamma d_f \mathbf{K}_f \nabla_{\mathcal{D}_f} u_{\mathcal{D}} \cdot \nabla_{\mathcal{D}_f} v_{\mathcal{D}} \, d\tau(\boldsymbol{x})$$

$$= \int_\Omega h_m \Pi_{\mathcal{D}_m} v_{\mathcal{D}} d\boldsymbol{x} + \int_\Gamma d_f h_f \Pi_{\mathcal{D}_f} v_{\mathcal{D}} d\tau(\boldsymbol{x}).$$

- Error estimate:

$$\|\nabla_{\mathcal{D}_m} u_{\mathcal{D}} - \nabla u\|_{L^2(\Omega)^d} + \|\nabla_{\mathcal{D}_f} u_{\mathcal{D}} - \nabla_\tau \gamma u\|_{L^2(\Gamma)^{d-1}}$$

$$+ \|\Pi_{\mathcal{D}_m} u_{\mathcal{D}} - u\|_{L^2(\Omega)} + \|\Pi_{\mathcal{D}_f} u_{\mathcal{D}} - \gamma u\|_{L^2(\Gamma)}$$

$$\leq C(C_{\mathcal{D}}, data)\Big(S_{\mathcal{D}}(u) + W_{\mathcal{D}}(\mathbf{q}_m, \mathbf{q}_f)\Big)$$

Gradient discretization of the hybrid dimensional Darcy flow model

Coercivity: (discrete Poincaré inequality)

$$C_{\mathcal{D}} = \max_{0 \neq v_{\mathcal{D}} \in X_{\mathcal{D}}^{0}} \frac{\|\Pi_{\mathcal{D}_m} v_{\mathcal{D}}\|_{L^2(\Omega)} + \|\Pi_{\mathcal{D}_f} v_{\mathcal{D}}\|_{L^2(\Gamma)}}{\|v_{\mathcal{D}}\|_{\mathcal{D}}}.$$

Consistency error: for all $u \in V^0$

$$S_{\mathcal{D}}(u) = \inf_{v_{\mathcal{D}} \in X_{\mathcal{D}}^{0}} \Big(\|\nabla_{\mathcal{D}_m} v_{\mathcal{D}} - \nabla u\|_{L^2(\Omega)^d} + \|\nabla_{\mathcal{D}_f} v_{\mathcal{D}} - \nabla_\tau \gamma u\|_{L^2(\Gamma)^{d-1}} + \|\Pi_{\mathcal{D}_m} v_{\mathcal{D}} - u\|_{L^2(\Omega)} + \|\Pi_{\mathcal{D}_f} v_{\mathcal{D}} - \gamma u\|_{L^2(\Gamma)} \Big),$$

Conformity error: for all $(\mathbf{q}_m, \mathbf{q}_f) \in W$

$$W_{\mathcal{D}}(\mathbf{q}_m, \mathbf{q}_f) = \sup_{0 \neq v_{\mathcal{D}} \in X_{\mathcal{D}}^{0}} \frac{1}{\|v_{\mathcal{D}}\|_{\mathcal{D}}} \left(\int_\Omega (\nabla_{\mathcal{D}_m} v_{\mathcal{D}} \cdot \mathbf{q}_m + (\Pi_{\mathcal{D}_m} v_{\mathcal{D}}) \mathrm{div}(\mathbf{q}_m))(\mathbf{x}) d\mathbf{x} + \int_\Gamma (\nabla_{\mathcal{D}_f} v_{\mathcal{D}} \cdot \mathbf{q}_f + \Pi_{\mathcal{D}_f} v_{\mathcal{D}} (\mathrm{div}_\tau(\mathbf{q}_f) + \mathbf{q}_m^+ \cdot \mathbf{n}^+ + \mathbf{q}_m^- \cdot \mathbf{n}^-))(\mathbf{x}) d\tau(\mathbf{x}) \right),$$

Vertex Approximate Gradient (VAG) and Hybrid Finite Volume (HFV) discretizations

VAG

- d.o.f. = cells v_K, fracture faces v_σ, and nodes v_s
- $\nabla_{\mathcal{D}_m} v_\mathcal{D}$: conforming $\mathbb{P}^1$ FE gradient on a tetrahedral submesh
- $\nabla_{\mathcal{D}_f} v_\mathcal{D}$: conforming $\mathbb{P}^1$ FE gradient on a triangular submesh

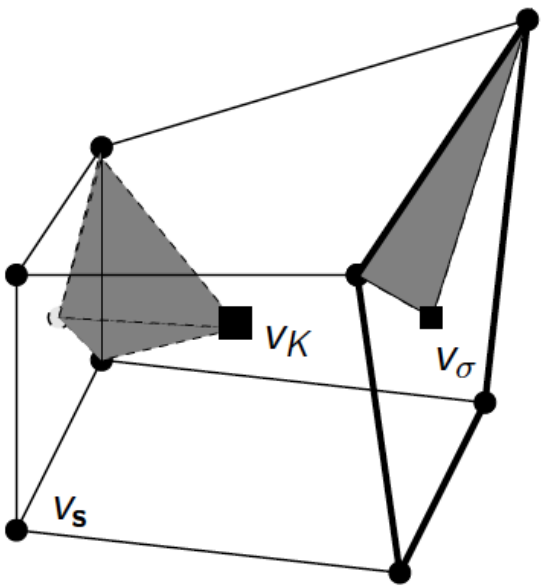

HFV

- d.o.f. = cells v_K, faces v_σ, and fracture edges v_e
- $\nabla_{\mathcal{D}_m} v_\mathcal{D}$: piecewise constant on a pyramidal submesh of K
- $\nabla_{\mathcal{D}_f} v_\mathcal{D}$: piecewise constant on triangular submesh of σ

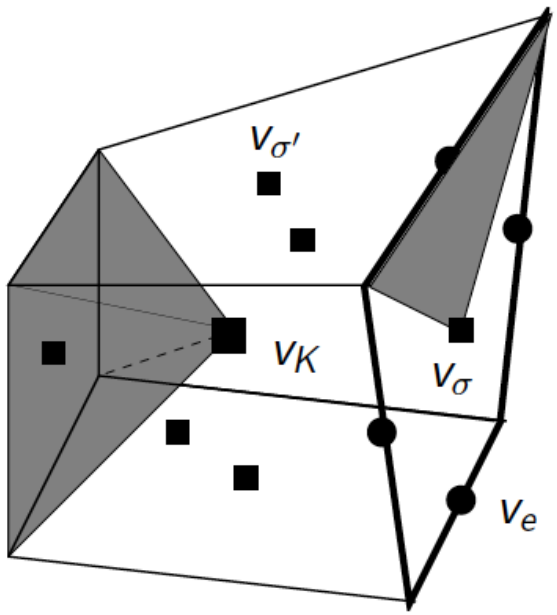

VAG and HFV Fluxes

- Matrix fluxes:
  - ∂K = d.o.f. at the boundary of K
  - $F_{K,\nu}(v_{\mathcal{D}}) = \sum_{\nu \in \partial_{\boldsymbol{K}}} T_K^{\nu,\nu'}(v_K - v_{\nu'})$
- Fracture fluxes:
  - $\partial \sigma$ = d.o.f. at the boundary of σ
  - $F_{\sigma,\nu}(v_{\mathcal{D}}) = \sum_{\nu' \in \partial_\sigma} T_\sigma^{\nu,\nu'}(v_\sigma - v_{\nu'})$

VAG HFV

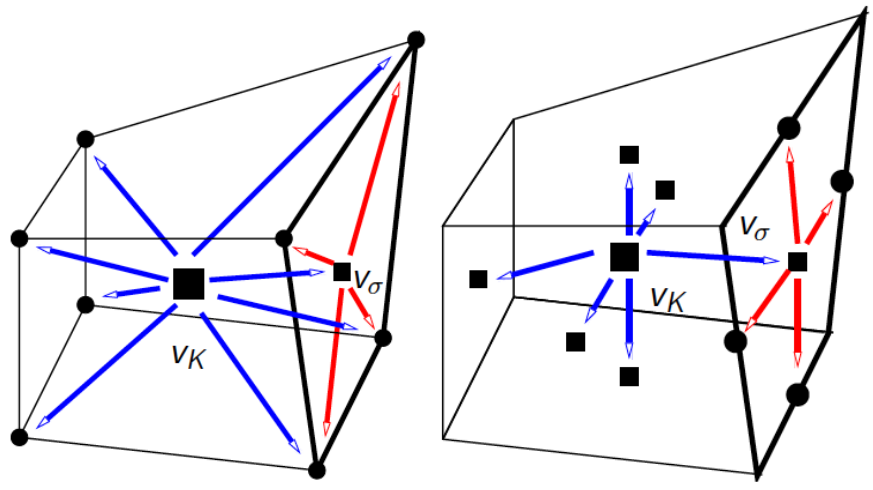

such that for all $w_{\mathcal{D}} \in V^0$:

$$\int_\Omega \mathbf{K}_m \nabla_{\mathcal{D}_m} v_{\mathcal{D}} \cdot \nabla_{\mathcal{D}_m} w_{\mathcal{D}} \, d\boldsymbol{x} + \int_\Gamma d_f \mathbf{K}_f \nabla_{\mathcal{D}_f} v_{\mathcal{D}} \cdot \nabla_{\mathcal{D}_f} w_{\mathcal{D}} \, d\tau$$

$$= \sum_{K \in \mathcal{M}} \sum_{\nu \in \partial_{\boldsymbol{K}}} F_{K,\nu}(v_{\mathcal{D}})(w_K - w_\nu) + \sum_{\sigma \in \mathcal{F}_\Gamma} \sum_{\nu \in \partial_\sigma} F_{\sigma,\nu}(v_{\mathcal{D}})(w_\sigma - w_\nu)$$

Choices of $\Pi_{\mathcal{D}_m}$ and $\Pi_{\mathcal{D}_f}$: Control Volumes

- $\Pi_{\mathcal{D}_m} v_{\mathcal{D}}$: piecewise constant on cell submeshes:

$$K = \omega_K \bigcup_{\nu \in \partial K \setminus dof_{Dir}} \omega_{K,\nu}$$

- $\Pi_{\mathcal{D}_f} v_{\mathcal{D}}$: piecewise constant on fracture face submeshes:

$$\sigma = \omega_\sigma \bigcup_{\nu \in \partial \sigma \setminus dof_{Dir}} \omega_{\sigma,\nu}$$

Practical choice is made to avoid the mixing of rocktypes at interfaces:

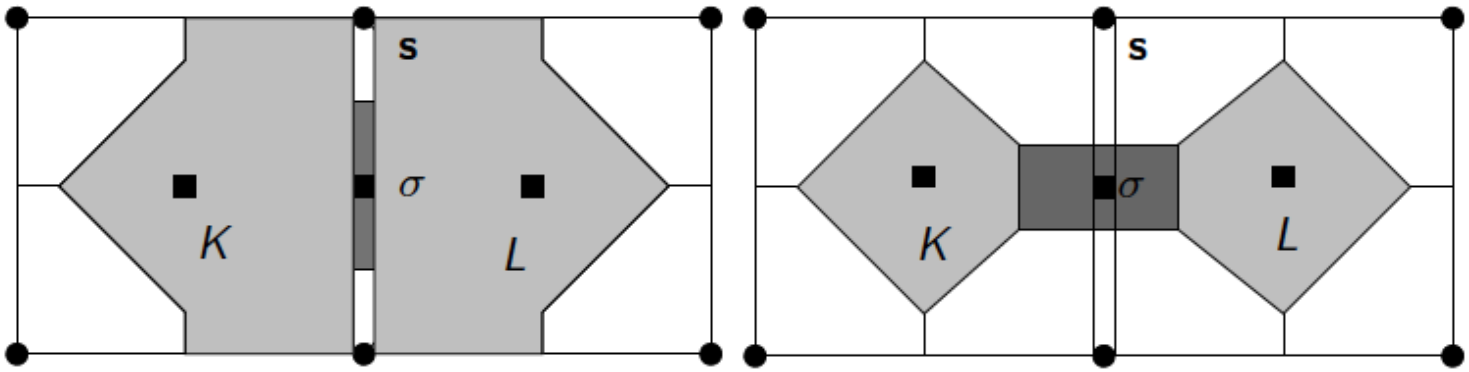

Good choice: VAG1 Bad choice (CVFE like): VAG2

Nb: only the volume distribution coefficients are needed

Finite Volume Formulation of VAG and HFV: discrete conservation laws on control volumes

Degrees of freedom: $dof = \mathcal{M} \cup \mathcal{F}_\Gamma \cup dof_{Dir} \cup \Big(dof \setminus (\mathcal{M} \cup \mathcal{F}_\Gamma \cup dof_{Dir}) \Big)$

$$\sum_{\nu \in \partial K} F_{K,\nu}(u_\mathcal{D}) = \int_{\omega_{\boldsymbol{K}}} h_m(\boldsymbol{x}) d\boldsymbol{x}, \;\; K \in \mathcal{M}$$

$$\sum_{\nu \in \partial \sigma} F_{\sigma,\nu}(u_\mathcal{D}) + \sum_{K \in \mathcal{M}_\sigma} -F_{K,\sigma}(u_\mathcal{D}) = \int_{\omega_\sigma} h_f(\boldsymbol{x}) d_f(\boldsymbol{x}) d\tau(\boldsymbol{x}) + \sum_{K \in \mathcal{M}_\sigma} \int_{\omega_{\boldsymbol{K},\sigma}} h_m(\boldsymbol{x}) d\boldsymbol{x}, \;\; \sigma \in \mathcal{F}_\Gamma,$$

$$\sum_{K \in \mathcal{M}_\nu} -F_{K,\nu}(u_\mathcal{D}) + \sum_{\sigma \in \mathcal{F}_{\Gamma,\nu}} -F_{\sigma,\nu}(u_\mathcal{D}) = \sum_{K \in \mathcal{M}_\nu} \int_{\omega_{\boldsymbol{K},\nu}} h_m(\boldsymbol{x}) d\boldsymbol{x} + \sum_{\sigma \in \mathcal{F}_{\Gamma,\nu}} \int_{\omega_{\sigma,\nu}} h_f(\boldsymbol{x}) d_f(\boldsymbol{x}) d\tau(\boldsymbol{x}), \;\; \nu \in dof \setminus (\mathcal{M} \cup \mathcal{F}_\Gamma \cup dof_{Dir}),$$

$$u_\nu = \overline{u}_\nu, \;\; \nu \in dof_{Dir}.$$

VAG discretization : comparison with CVFE (Bastian et al 2006, Firozabadi et al 2007)

- Matrix fluxes local to the cell and fracture fluxes local to the face
- Coercive fluxes not depending on the choice of the control volumes
- Choice of the control volumes to respect material interfaces
- Still maintain a "nodal" approach due to the elimination of the cell unknowns

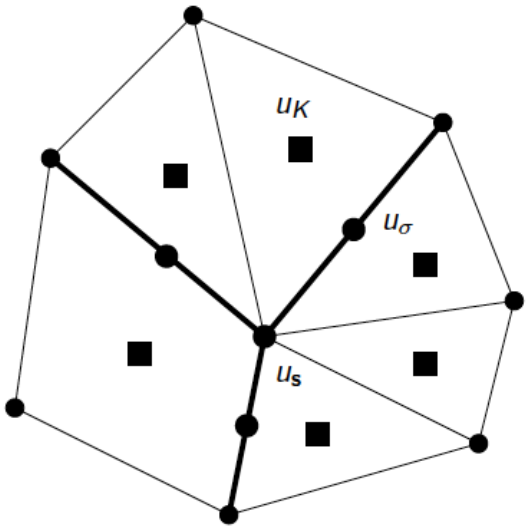

VAG

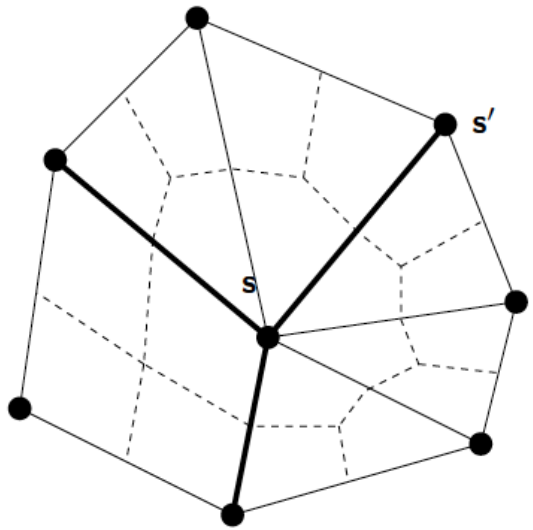

CVFE

Comparison of VAG and HFV schemes on hexahedral meshes

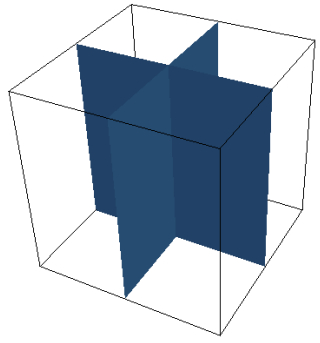

Heterogeneous Isotropic

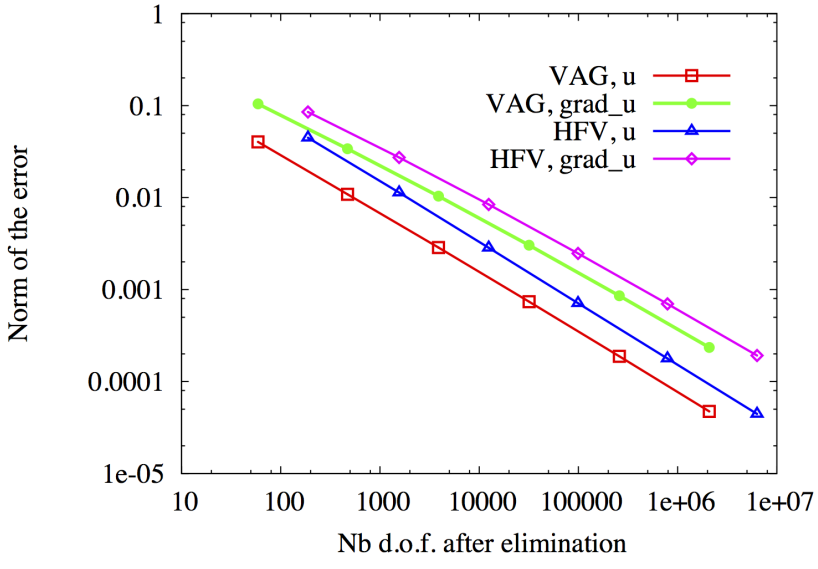

Heterogeneous anisotropic

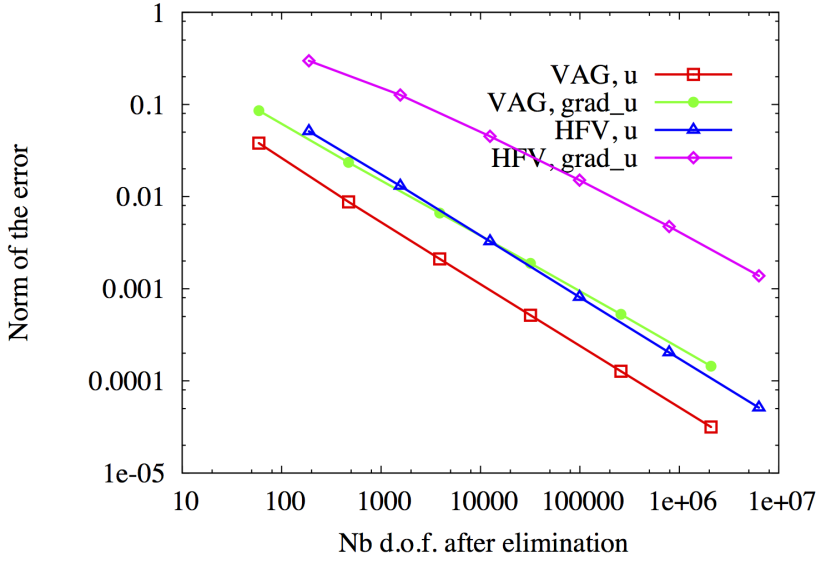

Comparison of VAG and HFV schemes on hexahedral meshes

	Isotropic case, Cartesian							***Anisotropic case, Cartesian***						
Vertex Approximate Gradient Discretization														
Nb	**It**	**F**	**Err$_u$**	**Err$_g$**	**CR$_u$**	**CR$_g$**	**CPU**	**It**	**F**	**Err$_u$**	**Err$_g$**	**CR$_u$**	**CR$_g$**	**CPU**
1	3	1.2	0.04	0.11	n/a	n/a	$1{\cdot}10^{-4}$	3	1.2	0.04	0.09	n/a	n/a	$8{\cdot}10^{-4}$
2	5	2.1	0.01	0.03	1.89	1.62	$7{\cdot}10^{-3}$	5	1.9	0.01	0.02	2.12	1.87	$6{\cdot}10^{-3}$
3	9	2.4	$2{\cdot}10^{-3}$	$1{\cdot}10^{-2}$	1.92	1.71	0.01	9	2.2	$2{\cdot}10^{-3}$	$6{\cdot}10^{-3}$	2.06	1.83	$8{\cdot}10^{-2}$
4	16	2.5	$7{\cdot}10^{-4}$	$3{\cdot}10^{-3}$	1.95	1.77	0.9	14	2.1	$5{\cdot}10^{-4}$	$2{\cdot}10^{-3}$	2.03	1.81	0.7
5	30	2.5	$2{\cdot}10^{-4}$	$8{\cdot}10^{-4}$	1.97	1.82	9	20	2.2	$1{\cdot}10^{-4}$	$5{\cdot}10^{-4}$	2.02	1.84	5
6	56	2.5	$5{\cdot}10^{-3}$	$2{\cdot}10^{-4}$	1.89	1.86	90	29	2.2	$3{\cdot}10^{-5}$	$1{\cdot}10^{-4}$	2.01	1.87	48
Hybrid Finite Volume Discretization														
Nb	**It**	**F**	**Err$_u$**	**Err$_g$**	**CR$_u$**	**CR$_g$**	**CPU**	**It**	**F**	**Err$_u$**	**Err$_g$**	**CR$_u$**	**CR$_g$**	**CPU**
1	6	3.3	0.01	0.04	n/a	n/a	$1.5{\cdot}10^{-3}$	4	2.5	0.01	0.16	n/a	n/a	$8{\cdot}10^{-4}$
2	10	3.6	$3{\cdot}10^{-3}$	0.02	1.98	1.64	$1.5{\cdot}10^{-2}$	6	3.1	$3{\cdot}10^{-3}$	0.05	1.97	1.23	$10{\cdot}10^{-3}$
3	17	3.6	$7{\cdot}10^{-4}$	$3{\cdot}10^{-3}$	1.99	1.71	0.1	10	3.6	$8{\cdot}10^{-4}$	0.02	1.99	1.49	0.1
4	29	3.6	$2{\cdot}10^{-4}$	$9{\cdot}10^{-4}$	1.99	1.77	1.5	18	3.7	$2{\cdot}10^{-4}$	$6{\cdot}10^{-3}$	2.01	1.58	1.5
5	59	3.6	$4{\cdot}10^{-5}$	$3{\cdot}10^{-4}$	2	1.82	19	30	3.8	$5{\cdot}10^{-5}$	$2{\cdot}10^{-3}$	1.99	1.68	20
6	122	3.6	$1{\cdot}10^{-5}$	$7{\cdot}10^{-5}$	2	1.86	357	65	3.8	$1{\cdot}10^{-5}$	$5{\cdot}10^{-4}$	1.99	1.78	303

Comparison of VAG and HFV schemes on tetrahedral meshes

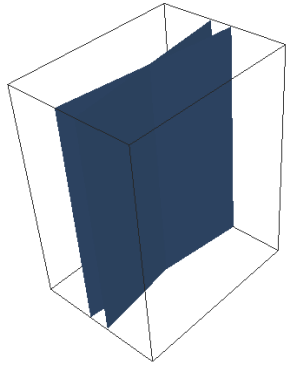

Heterogeneous Isotropic

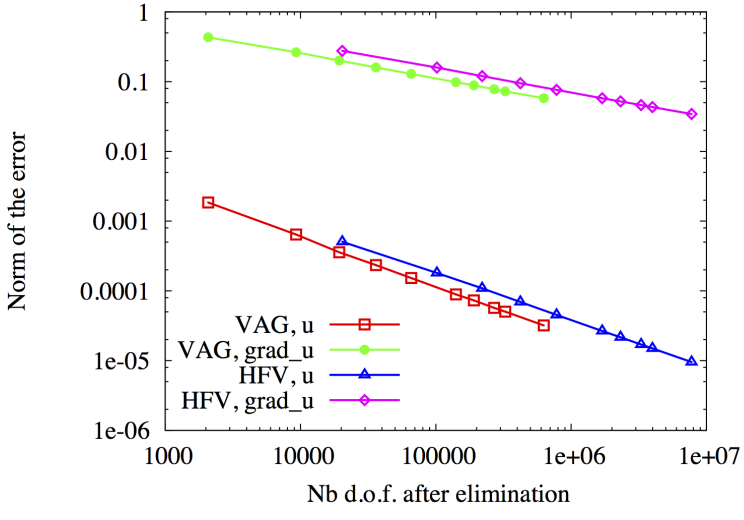

Heterogeneous anisotropic

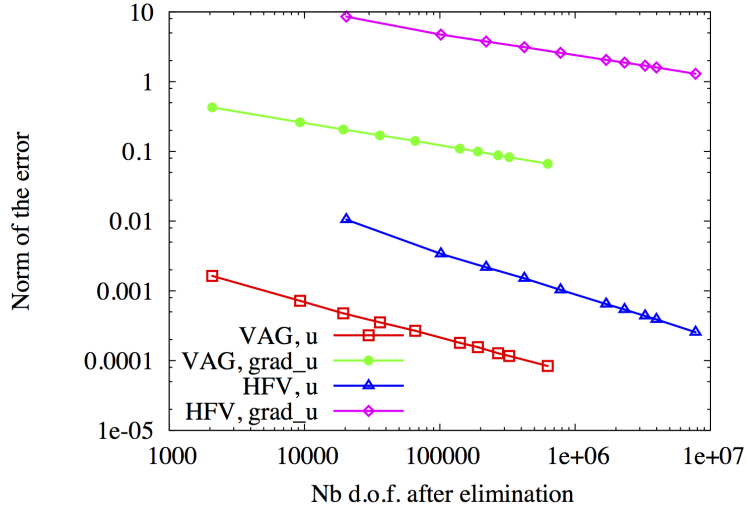

Comparison of VAG and HFV schemes on tetrahedral meshes

	Isotropic case							***Anisotropic case***						
Vertex Approximate Gradient Discretization														
Nb	**It**	**F**	**ErrF**	**Err$_g$**	**CR$_u$**	**CR$_g$**	**CPU**	**It**	**F**	**ErrF**	**Err$_g$**	**CR$_u$**	**CR$_g$**	**CPU**
1	11	2.5	$1.85{\cdot}10^{-3}$	0.43	n/a	n/a	$4{\cdot}10^{-2}$	13	2.5	$1.64{\cdot}10^{-3}$	0.42	n/a	n/a	$5{\cdot}10^{-2}$
2	32	2.7	$6.43{\cdot}10^{-4}$	0.26	1.96	0.91	0.3	20	2.8	$7.21{\cdot}10^{-4}$	0.26	1.52	0.91	0.3
3	51	2.8	$3.57{\cdot}10^{-4}$	0.20	2.28	1.06	0.7	52	2.8	$4.77{\cdot}10^{-4}$	0.21	1.60	0.92	0.8
4	51	2.8	$2.34{\cdot}10^{-4}$	0.16	1.94	1.05	1.7	51	2.9	$3.53{\cdot}10^{-4}$	0.17	1.38	0.89	2
5	51	2.9	$1.53{\cdot}10^{-4}$	0.13	2.07	1.04	3	51	2.9	$2.67{\cdot}10^{-4}$	0.14	1.35	0.89	4
6	51	2.9	$8.89{\cdot}10^{-5}$	$9.80{\cdot}10^{-2}$	2.08	1.06	8	51	2.9	$1.80{\cdot}10^{-4}$	0.11	1.53	0.98	9
7	51	2.9	$7.31{\cdot}10^{-5}$	$8.86{\cdot}10^{-2}$	1.88	0.97	10	51	2.9	$1.56{\cdot}10^{-4}$	$9.96{\cdot}10^{-2}$	1.37	0.88	13
8	52	2.9	$5.71{\cdot}10^{-5}$	$7.77{\cdot}10^{-2}$	2.12	1.12	17	53	2.9	$1.27{\cdot}10^{-4}$	$8.78{\cdot}10^{-2}$	1.73	1.08	18
9	60	2.9	$5.04{\cdot}10^{-5}$	$7.27{\cdot}10^{-2}$	1.95	1.03	22	56	2.9	$1.16{\cdot}10^{-4}$	$8.26{\cdot}10^{-2}$	1.41	0.95	23
10	78	2.9	$3.19{\cdot}10^{-5}$	$5.78{\cdot}10^{-2}$	2.04	1.03	46	72	3	$8.388{\cdot}10^{-5}$	$6.66{\cdot}10^{-2}$	1.48	0.97	49
Hybrid Finite Volume Discretization														
Nb	**It**	**F**	**ErrF**	**Err$_g$**	**CR$_u$**	**CR$_g$**	**CPU**	**It**	**F**	**ErrF**	**Err$_g$**	**CR$_u$**	**CR$_g$**	**CPU**
1	51	4.7	$5.06{\cdot}10^{-4}$	0.28	n/a	n/a	0.2	52	5.1	$1.05{\cdot}10^{-2}$	8.56	n/a	n/a	0.5
2	51	4.8	$1.81{\cdot}10^{-4}$	0.16	1.91	1.02	1.8	84	5.2	$3.39{\cdot}10^{-3}$	4.73	2.09	1.09	4
3	53	4.8	$1.09{\cdot}10^{-4}$	0.12	1.96	1.09	4.6	97	5.2	$2.18{\cdot}10^{-3}$	3.75	1.73	0.89	11
4	71	4.9	$6.94{\cdot}10^{-5}$	$9.49{\cdot}10^{-2}$	2.07	1.08	10	108	5.2	$1.51{\cdot}10^{-3}$	3.11	1.68	0.86	23
5	88	4.9	$4.53{\cdot}10^{-5}$	$7.62{\cdot}10^{-2}$	2.07	1.07	24	146	5.2	$1.03{\cdot}10^{-3}$	2.58	1.84	0.91	54
6	114	4.9	$2.66{\cdot}10^{-5}$	$5.79{\cdot}10^{-2}$	2.05	1.06	65	248	5.2	$6.47{\cdot}10^{-4}$	2.04	1.80	0.89	177
7	132	4.9	$2.16{\cdot}10^{-5}$	$5.21{\cdot}10^{-2}$	1.98	1.01	98	532	5.2	$5.41{\cdot}10^{-4}$	1.87	1.72	0.84	387
8	146	4.9	$1.69{\cdot}10^{-5}$	$4.61{\cdot}10^{-2}$	2.06	1.05	157	530	5.2	$4.37{\cdot}10^{-4}$	1.69	1.83	0.88	565
9	165	4.9	$1.49{\cdot}10^{-5}$	$4.32{\cdot}10^{-2}$	1.99	1.01	216	312	5.2	$3.89{\cdot}10^{-4}$	1.59	1.80	0.90	477
10	196	4.9	$9.54{\cdot}10^{-6}$	$3.43{\cdot}10^{-2}$	2.02	1.03	498	748	5.2	$2.55{\cdot}10^{-4}$	1.29	1.89	0.94	906

Extension to Two Phase Darcy flow using a pressure pressure formulation

- u^1, u^2: non wetting and wetting phase pressures,
- $p = u^1 - u^2$ capillary pressure,
- $S_m^\alpha(\boldsymbol{x}, p)$, $S_f^\alpha(\boldsymbol{x}, \gamma p)$: inverse of the capillary pressures in the matrix and in the fractures

Find $u^\alpha \in L^2(0, T; V^0)$, $(\mathbf{q}_m^\alpha, \mathbf{q}_f^\alpha) \in L^2(0, T; \mathbf{W})$, $\alpha = 1, 2$, such that for $\alpha = 1, 2$:

$$
\begin{cases}
\phi_m \partial_t \left(S_m^\alpha(\boldsymbol{x}, p) \right) + \operatorname{div}(\mathbf{q}_m^\alpha) = 0 & \text{on } \Omega \setminus \overline{\Gamma}, \\
\phi_f d_f \partial_t \left(S_f^\alpha(\boldsymbol{x}, \gamma p) \right) + \operatorname{div}_\tau(\mathbf{q}_f^\alpha) + \mathbf{q}_m^{\alpha,+} \cdot \mathbf{n}^+ + \mathbf{q}_m^{\alpha,-} \cdot \mathbf{n}^- = 0 & \text{on } \Gamma, \\
-\dfrac{k_{r,m}^\alpha(\boldsymbol{x}, S_m^\alpha(\boldsymbol{x}, p))}{\mu^\alpha} \mathbf{K}_m \nabla u^\alpha = \mathbf{q}_m^\alpha & \text{on } \Omega \setminus \overline{\Gamma}, \\
-\dfrac{k_{r,f}^\alpha(\boldsymbol{x}, S_f^\alpha(\boldsymbol{x}, \gamma p))}{\mu^\alpha} d_f \mathbf{K}_f \nabla_\tau \gamma u^\alpha = \mathbf{q}_f^\alpha & \text{on } \Gamma, \\
p|_{t=0} = p_{\text{ini}}, & \text{on } \Omega,
\end{cases}
$$

Variational formulation in $L^2(0, T; V^0)$

The weak formulation amounts to find $u^\alpha \in L^2(0, T; V^0)$, $\alpha = 1, 2$, such that for all $v^\alpha \in C_c^\infty([0, T[\times\Omega)$ and $\alpha = 1, 2$, one has:

$$
\begin{cases}
\displaystyle\int_0^T \int_\Omega \left(-\phi_m S_m^\alpha(\boldsymbol{x}, p) \partial_t v^\alpha + \frac{k_{r,m}^\alpha(\boldsymbol{x}, S_m^\alpha(\boldsymbol{x}, p))}{\mu^\alpha} \mathbf{K}_m \nabla u^\alpha \cdot \nabla v^\alpha \right) d\boldsymbol{x} dt \\
\displaystyle + \int_0^T \int_\Gamma -\phi_f d_f \; S_f^\alpha(\boldsymbol{x}, \gamma p) \; \partial_t \gamma v^\alpha \; d\tau(\boldsymbol{x}) dt \\
\displaystyle + \int_0^T \int_\Gamma \frac{k_{r,f}^\alpha(\boldsymbol{x}, S_f^\alpha(\boldsymbol{x}, \gamma p))}{\mu^\alpha} \; d_f \mathbf{K}_f \nabla_\tau \gamma u^\alpha \cdot \nabla_\tau \gamma v^\alpha \; d\tau(\boldsymbol{x}) dt \\
\displaystyle - \int_\Omega \phi_m S_m^\alpha(\boldsymbol{x}, p_{\text{ini}}) v^\alpha(\boldsymbol{x}, 0) \; d\boldsymbol{x} dt - \int_\Gamma \phi_f d_f S_f^\alpha(\boldsymbol{x}, \gamma p_{\text{ini}}) v^\alpha(\boldsymbol{x}, 0) \; d\tau(\boldsymbol{x}) dt = 0.
\end{cases}
$$

Gradient discretization: phase pressures variational formulation, Euler implicit time integration

$u_{\mathcal{D}}^{\alpha} = \left(u_{\mathcal{D}}^{\alpha,n} \in X_{\mathcal{D}}^0\right)_{n=1,\cdots,N}$, $\alpha = 1,2$, such that for $\alpha = 1,2$, and for all $v_{\mathcal{D}}^{\alpha} \in X_{\mathcal{D}}^0$ one has

$$\int_\Omega \phi_m \frac{S_{\mathcal{D}_m}^{\alpha,n} - S_{\mathcal{D}_m}^{\alpha,n-1}}{\Delta t^n} \Pi_{\mathcal{D}_m} v_{\mathcal{D}}^{\alpha} \, d\boldsymbol{x} + \int_\Omega \frac{k_{\mathcal{D}_m}^{\alpha,n}}{\mu^\alpha} \mathbf{K}_m \nabla_{\mathcal{D}_m} u_{\mathcal{D}}^{\alpha,n} \cdot \nabla_{\mathcal{D}_m} v_{\mathcal{D}}^{\alpha} \, d\boldsymbol{x} +$$

$$\int_\Gamma \phi_f d_f \frac{S_{\mathcal{D}_f}^{\alpha,n} - S_{\mathcal{D}_f}^{\alpha,n-1}}{\Delta t^n} \Pi_{\mathcal{D}_f} v_{\mathcal{D}}^{\alpha} \, d\tau(\boldsymbol{x}) + \int_\Gamma \frac{k_{\mathcal{D}_f}^{\alpha,n}}{\mu^\alpha} d_f \mathbf{K}_f \nabla_{\mathcal{D}_f} u_{\mathcal{D}}^{\alpha,n} \cdot \nabla_{\mathcal{D}_f} v_{\mathcal{D}}^{\alpha} \, d\tau(\boldsymbol{x}) = 0.$$

using with $p_{\mathcal{D}}^n = u_{\mathcal{D}}^{1,n} - u_{\mathcal{D}}^{2,n} \in X_{\mathcal{D}}^0$

$$S_{\mathcal{D}_m}^{\alpha,n}(\boldsymbol{x}) = S_m^\alpha(\boldsymbol{x}, \Pi_{\mathcal{D}_m} p_{\mathcal{D}}^n(\boldsymbol{x})), \;\; S_{\mathcal{D}_f}^{\alpha,n}(\boldsymbol{x}) = S_f^\alpha(\boldsymbol{x}, \Pi_{\mathcal{D}_f} p_{\mathcal{D}}^n(\boldsymbol{x})),$$

and

$$k_{\mathcal{D}_m}^{\alpha,n}(\boldsymbol{x}) = k_{r,m}^\alpha(\boldsymbol{x}, S_{\mathcal{D}_m}^{\alpha,n}(\boldsymbol{x})), \;\; k_{\mathcal{D}_f}^{\alpha,n}(\boldsymbol{x}) = k_{r,f}^\alpha(\boldsymbol{x}, S_{\mathcal{D}_f}^{\alpha,n}(\boldsymbol{x})),$$

Convergence

Weak convergence of the pressures and strong convergence of the saturations:

- assuming consistency, coercivity, limit conformity, and compacity properties of the operators
- assuming non vanishing relative permeabilities

Practical VAG or HFV Discretizations of two phase Darcy flows

- Conservation equations in the control volumes using the Darcy fluxes
- Discretization of the saturations function of $p_{\mathcal{D}} = u^1_{\mathcal{D}} - u^2_{\mathcal{D}}$

$$\left\{ \begin{array}{r} S^\alpha_{K,\nu} = S^\alpha_m(\boldsymbol{x}_K, p_\nu), \\ S^\alpha_K = S^\alpha_m(\boldsymbol{x}_K, p_K), \end{array} \right. \qquad \left\{ \begin{array}{r} S^\alpha_{\sigma,\mathbf{s}} = S^\alpha_f(\boldsymbol{x}_\sigma, p_\mathbf{s}), \\ S^\alpha_\sigma = S^\alpha_f(\boldsymbol{x}_\sigma, p_\sigma). \end{array} \right.$$

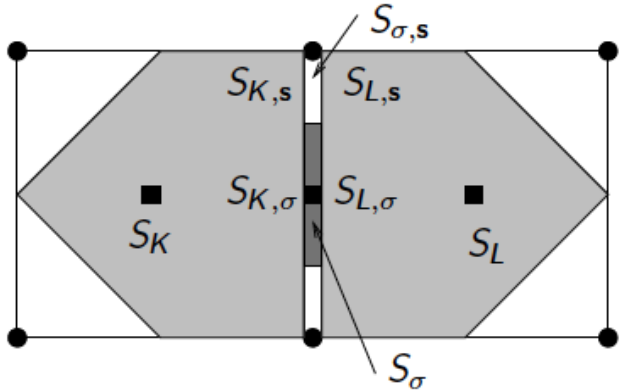

- Upwinding of the relative permeabilities between K and (K,ν) and between σ and (σ,ν)

$$\left\{ \begin{array}{l} V^\alpha_{K,\nu}(u^{\alpha,n}_{\mathcal{D}}) = \dfrac{k^\alpha_{r,m}(\boldsymbol{x}_K, S^{\alpha,n}_K)}{\mu^\alpha} F_{K,\nu}(u^{\alpha,n}_{\mathcal{D}})^+ + \dfrac{k^\alpha_{r,m}(\boldsymbol{x}_K, S^{\alpha,n}_{K,\nu})}{\mu^\alpha} F_{K,\nu}(u^{\alpha,n}_{\mathcal{D}})^- \\ V^\alpha_{\sigma,\nu}(u^{\alpha,n}_{\mathcal{D}}) = \dfrac{k^\alpha_{r,f}(\boldsymbol{x}_\sigma, S^{\alpha,n}_\sigma)}{\mu^\alpha} F_{\sigma,\mathbf{s}}(u^{\alpha,n}_{\mathcal{D}})^+ + \dfrac{k^\alpha_{r,f}(\boldsymbol{x}_\sigma, S^{\alpha,n}_{\sigma,\mathbf{s}})}{\mu^\alpha} F_{\sigma,\mathbf{s}}(u^{\alpha,n}_{\mathcal{D}})^- \end{array} \right.$$

Practical VAG or HFV Discretizations of two phase Darcy flows: discrete conservation equations

Degrees of freedom: $dof = \mathcal{M} \cup \mathcal{F}_\Gamma \cup dof_{Dir} \cup \Big(dof \setminus (\mathcal{M} \cup \mathcal{F}_\Gamma \cup dof_{Dir}) \Big)$

$$\frac{\phi_K (S_K^{\alpha,n} - S_K^{\alpha,n-1})}{\Delta t^n} |\omega_K| + \sum_{\nu \in \partial K} V_{K,\nu}^\alpha (u_\mathcal{D}^{\alpha,n}) = 0, \ K \in \mathcal{M}$$

$$\frac{\phi_\sigma (S_\sigma^{\alpha,n} - S_\sigma^{\alpha,n-1})}{\Delta t^n} d_\sigma |\omega_\sigma| + \sum_{\nu \in \partial \sigma} V_{\sigma,\nu}^\alpha (u_\mathcal{D}^{\alpha,n}) + \sum_{K \in \mathcal{M}_\sigma} -V_{K,\nu}^\alpha (u_\mathcal{D}^{\alpha,n}) = 0, \ \sigma \in \mathcal{F}_\Gamma,$$

$$\sum_{K \in \mathcal{M}_\nu} \frac{\phi_K (S_{K,\nu}^{\alpha,n} - S_{K,\nu}^{\alpha,n-1})}{\Delta t^n} |\omega_{K,\nu}| + \sum_{\sigma \in \mathcal{F}_{\Gamma,\nu}} \frac{\phi_\sigma (S_{\sigma,\nu}^{\alpha,n} - S_{\sigma,\nu}^{\alpha,n-1})}{\Delta t^n} d_\sigma |\omega_{\sigma,\nu}|$$
$$+ \sum_{K \in \mathcal{M}_\nu} -V_{K,\nu}^\alpha (u_\mathcal{D}^{\alpha,n}) + \sum_{\sigma \in \mathcal{F}_{\Gamma,\nu}} -V_{\sigma,\nu}^\alpha (u_\mathcal{D}^{\alpha,n}) = 0, \ \nu \in dof \setminus (\mathcal{M} \cup \mathcal{F}_\Gamma \cup dof_{Dir}),$$

$$u_\nu^{\alpha,n} = \overline{u}_\nu^{\alpha,n}, \ \nu \in dof_{Dir}.$$

Oil migration by gravity from the bottom boundary in a 3D basin initially saturated with water

Incompressible - Immiscible two phase Darcy flow

$d_f = 0.01$ m, $L = H = 100$ m, $\frac{K_f}{K_m} = 10^6$

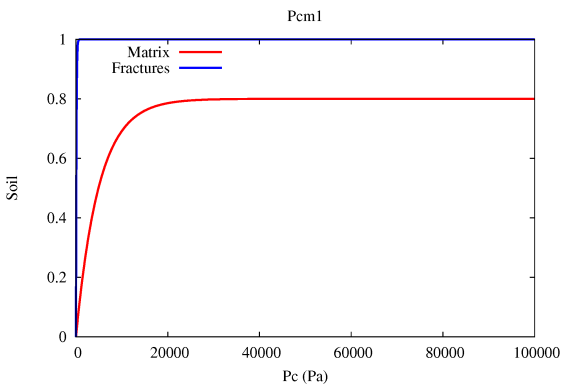

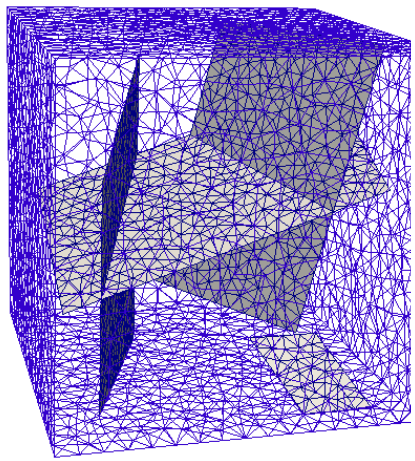

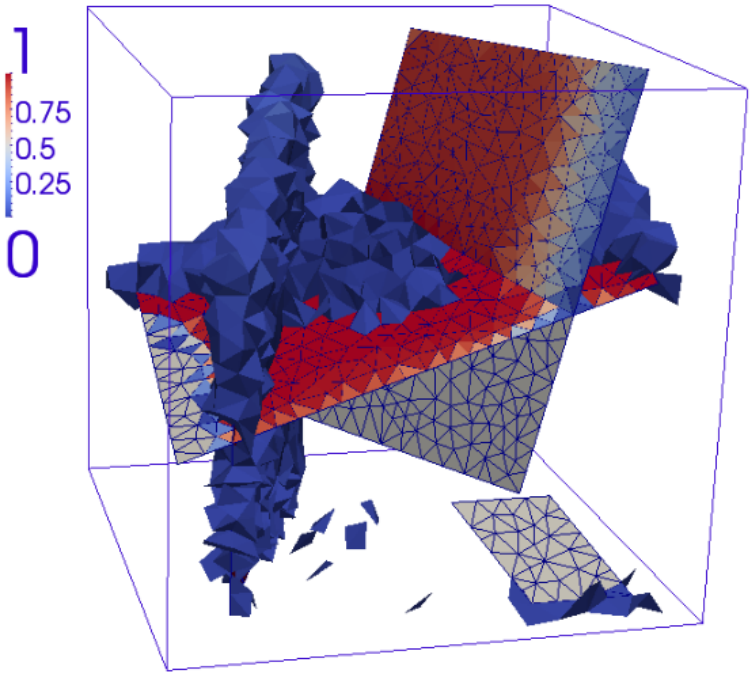

Oil migration by gravity: oil saturation for $\frac{K_f}{K_m} = 10^3$

Loading video...

VAG1 and VAG2 comparison: $\frac{K_f}{K_m} = 10^6$

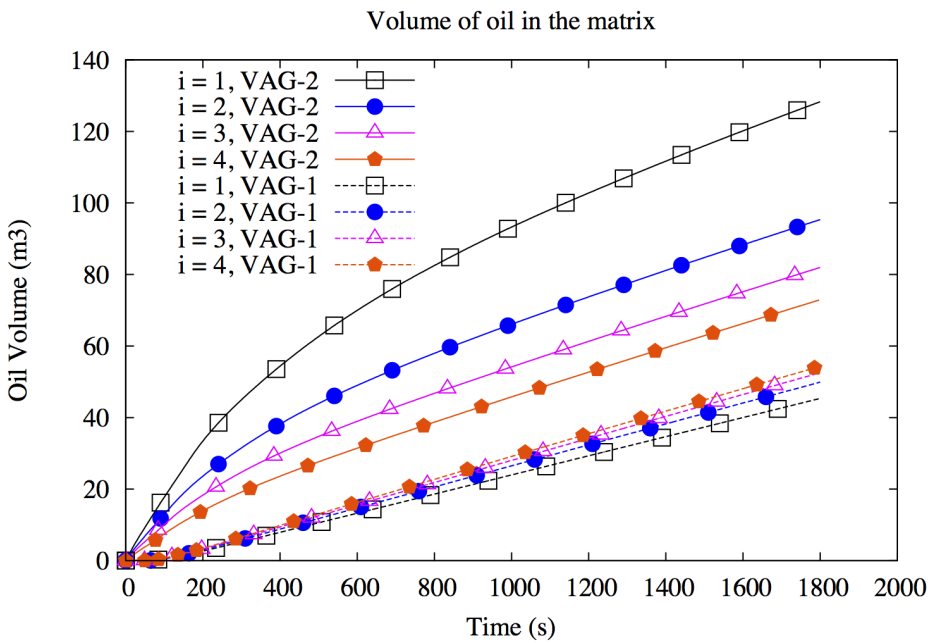

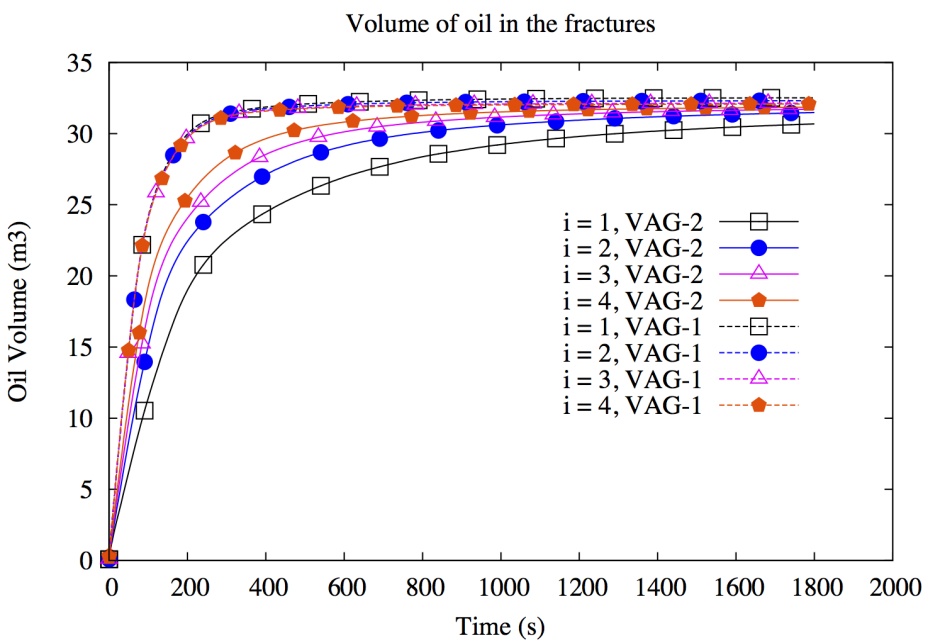

Meshes and numerical behavior: $\frac{K_f}{K_m} = 10^6$

Discretization properties:

Nb_{cells}	Nb_{nodes}	Nb_{FracF}	linear system d.o.f.
47 670	8 348	1 678	9 278
253 945	41 043	6 655	46 283
837 487	132 778	16 497	147 148
3 076 262	483 786	42 966	523 453

Numerical behavior: VAG1 vs VAG2

Volumes	$N_{\Delta t}$	N_{Chop}	N_{Newton}	N_{GMRes}	CPU (s)
VAG-1	384	6	2.20	10.05	590
VAG-1	390	10	3.08	15.11	5 900
VAG-1	415	21	4.02	15.93	31 800
VAG-1	784	30	3.37	16.75	209 500
VAG-2	373	0	1.87	6.94	480
VAG-2	373	0	2.42	13.05	4 450
VAG-2	375	1	3.02	14.56	21 600
VAG-2	747	13	2.92	16.55	173 000

VAG vs HFV: $\frac{K_f}{K_m} = 10^6$

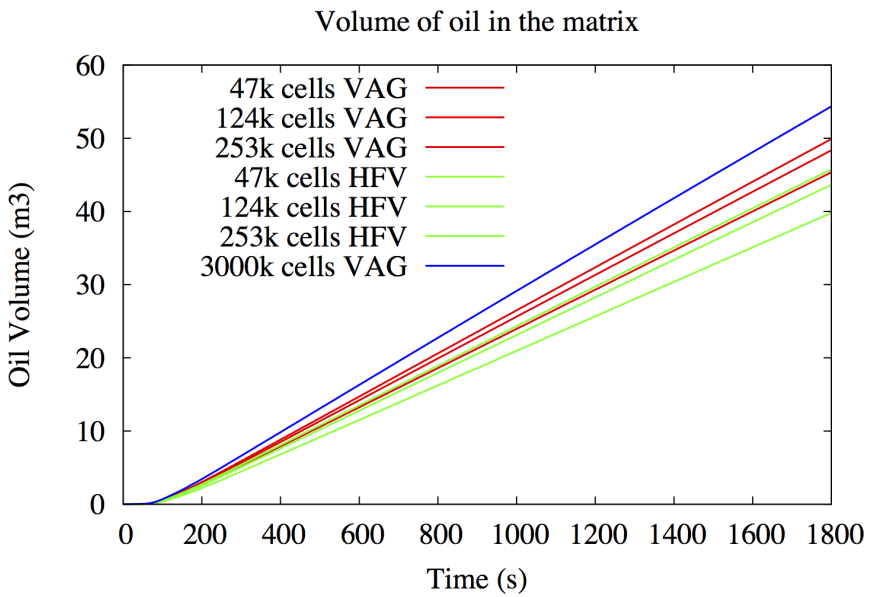

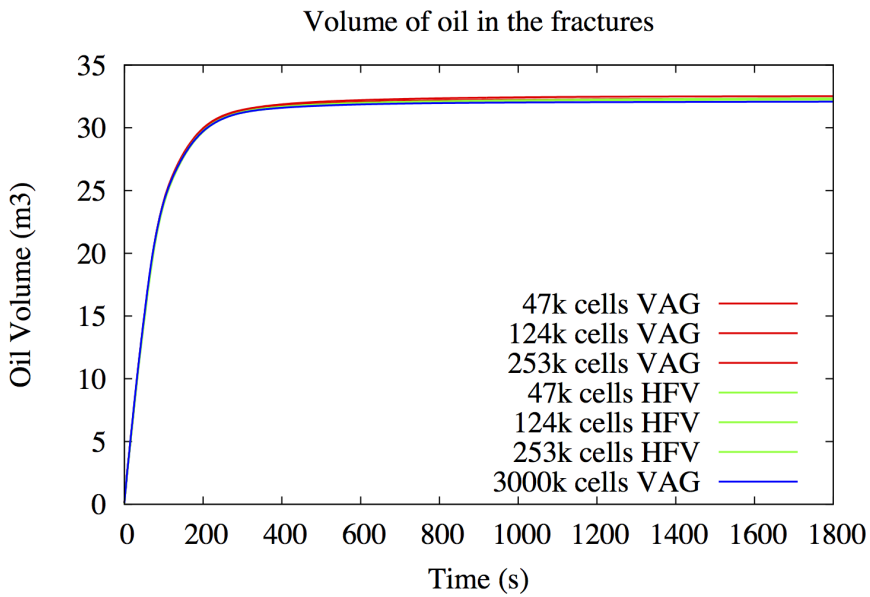

VAG vs HFV: $\frac{K_f}{K_m} = 10^6$

Numerical behavior: VAG vs HFV

Scheme	N_{Cells}	dof	N_{zeros}	$N_{\Delta t}$	N_{Chop}	N_{Newton}	N_{GMRes}	CPU (s)
VAG	47k	9k	130k	384	6	2.2	10	590
VAG	124k	23k	338k	391	8	2.5	11	2000
VAG	253k	46k	686k	390	10	3.1	15	5900
HFV	47k	98k	682k	385	10	2.9	20	4900
HFV	124k	254k	1777k	413	20	3.9	34	25000
HFV	253k	517k	3628k	449	33	4.9	47	95000

Oil migration in a 2D network: oil saturation for $\frac{K_f}{K_m} = 10^4$

Loading video...

Oil migration in a 2D network: oil saturation for $\frac{K_f}{K_m} = 10^2$

Loading video...

Oil migration in a 2D network

$\frac{K_f}{K_m} = 10^2$

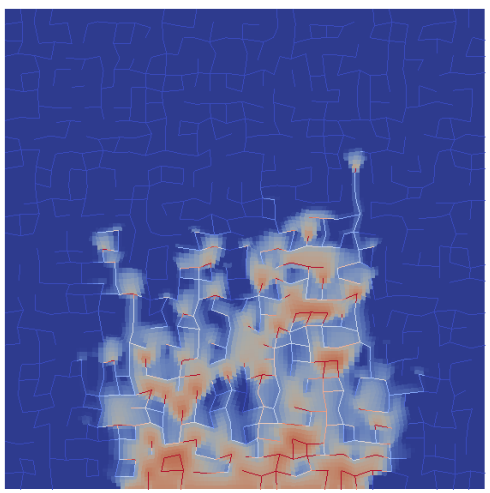

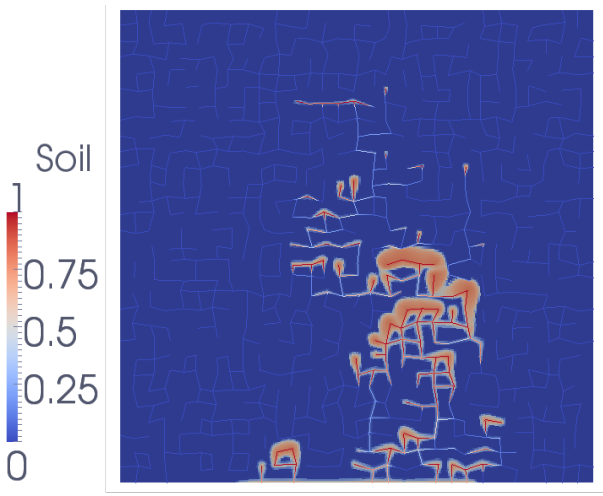

$\frac{K_f}{K_m} = 10^4$

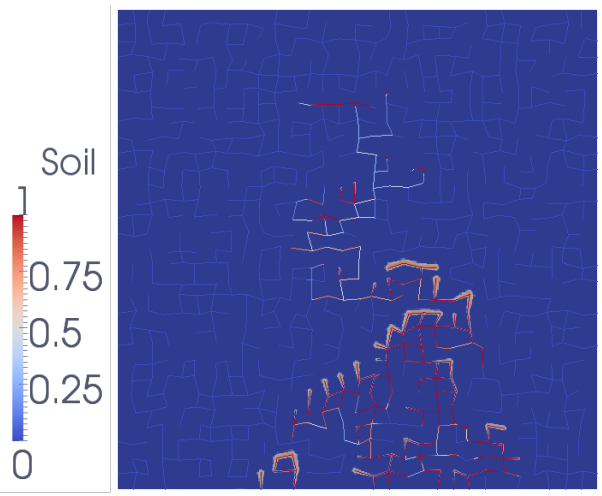

$\frac{K_f}{K_m} = 10^6$

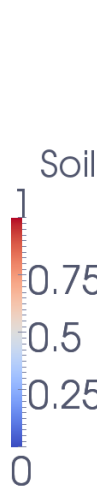

Gaz liquid two-phase compositional Darcy flow example

Gas component molar fraction in the liquid phase and gaz saturation:

Loading video...

Conclusion and perspectives

- Gradient scheme framework for hybrid dimensional Darcy flows for DFN models (continuous pressure)
  - Convergence proof for single and two phase flows
- VAG discretization: outperforms CVFE discretizations for high permeability ratio $\frac{K_f}{K_m}$
- Roughly a factor 10 in CPU time between HFV and VAG on tetrahedral meshes
- On going work:
  - other formulations than pressure pressure
  - extension to discontinuous pressure models